

# Age-related Dendritic and Spine Changes in Corticocortically Projecting Neurons in Macaque Monkeys

Huilong Duan<sup>1,2</sup>, Susan L. Wearne<sup>2,3,5</sup>, Anne B. Rocher<sup>1,2</sup>, Aisha Macedo<sup>1,2</sup>, John H. Morrison<sup>1,2,4,5</sup> and Patrick R. Hof<sup>1,2,4,5</sup>

<sup>1</sup>Kastor Neurobiology of Aging Laboratories, <sup>2</sup>Fishberg Research Center for Neurobiology, <sup>3</sup>Department of Biomathematical Sciences, <sup>4</sup>Department of Geriatrics and Adult Development and <sup>5</sup>Advanced Imaging Program, Mount Sinai School of Medicine, New York, NY 10029, USA

**Alterations in neuronal morphology occur in primate cerebral cortex during normal aging, vary depending on the neuronal type, region and cortical layer, and have been related to memory and cognitive impairment. We analyzed how such changes affect a specific subpopulation of cortical neurons forming long corticocortical projections from the superior temporal cortex to prefrontal area 46. These neurons were identified by retrograde transport in young and old macaque monkeys. Dendritic arbors of retrogradely labeled neurons were visualized in brain slices by intracellular injection of Lucifer Yellow, and reconstructed three-dimensionally using computer-assisted morphometry. Total dendritic length, numbers of segments, numbers of spines, and spine density were analyzed in layer III pyramidal neurons forming the projection considered. Sholl analysis was used to determine potential age-related changes in dendritic complexity. We observed statistically significant age-related decreases in spine numbers and density on both apical and basal dendritic arbors in these projection neurons. On apical dendrites, changes in spine numbers occurred mainly on the proximal dendrites but spine density decreased uniformly among the different branch orders. On basal dendrites, spine numbers and density decreased preferentially on distal branches. Regressive dendritic changes were observed only in one particular portion of the apical dendrites, with the general dendritic morphology and extent otherwise unaffected by aging. In view of the fact that there is no neuronal loss in neocortex and hippocampus in old macaque monkeys, it is possible that the memory and cognitive decline known to occur in these animals is related to rather subtle changes in the morphological and molecular integrity of neurons subserving identifiable neocortical association circuits that play a critical role in cognition.**

## Introduction

Neocortical function is relying on the cohesive activity of large-scale networks of functionally interconnected association regions (Jones and Powell, 1970; Goldman-Rakic, 1988; Bressler, 1995; Mesulam, 1998). *In vivo* tract-tracing studies in non-human primates have revealed widely distributed networks of interconnected cortical areas [for reviews see (Felleman and Van Essen, 1991; Young, 1993; Hof *et al.*, 1995)]. Among them, the long distance corticocortical bidirectional pathways between unimodal and multimodal temporoparietal neocortical areas and supramodal prefrontal areas, especially over the dorsolateral prefrontal region, are believed to mediate cognitive processes, including memory (Goldman-Rakic, 1988; Fuster, 1997; Mesulam, 1998; Miller and Cohen, 2001).

It is well known that cognitive abilities are impaired during normal aging (Moscovitch and Winocur, 1995; West, 1996; Gallagher and Rapp, 1997; Rapp and Gallagher, 1997). To date, however, the neurobiological factors underlying such age-related cognitive decline remain largely unknown. Although it has been proposed that cognitive decline arises from widespread and substantial loss of cortical neurons, current evidence suggests that the number of cortical neurons is largely preserved in aged

macaque monkeys and humans (Peters *et al.*, 1996; Gazzaley *et al.*, 1997; Morrison and Hof, 1997; Peters *et al.*, 1998a; Hof *et al.*, 2000). Furthermore, recent studies failed to detect an age-related decrease in cortical volume in area 46 (O'Donnell *et al.*, 1999) and area 17 (Peters *et al.*, 1997). These data suggest that a higher resolution investigation of more subtle cellular alterations may be required to reveal neurological indices that account for the observed deficits. A number of studies have shown that the dendritic arbors and the dendritic spines of cortical pyramidal neurons undergo age-related regressive changes in specific regions and layers of human and non-human primate cortex (Scheibel *et al.*, 1975; Cupp and Uemura, 1980; Uemura, 1980; Nakamura *et al.*, 1985; Jacobs and Scheibel, 1993; Anderson and Rutledge, 1996; Jacobs *et al.*, 1997; de Brabander *et al.*, 1998; Peters *et al.*, 1998b, 2001). In the prefrontal cortex, such dendritic and spine alterations have been correlated with impairments of memory and cognitive function in macaque monkeys (Peters *et al.*, 1998b). In this context, we have recently reported a decreased expression of ionotropic glutamate receptor subunit proteins in neocortical projection neurons in aged macaque and Patas monkeys (Hof *et al.*, 2002). We proposed that these alterations in the molecular complement of glutamate receptors result from age-related changes in the dendrites or spines of these projection neurons. Preliminary data have in fact demonstrated the existence of regressive dendritic and spine changes in identified, corticocortically projecting neurons in aged monkeys (Duan *et al.*, 2000; Page *et al.*, 2002).

The distribution of the neurons of origin of long association pathways in the macaque monkey neocortex is well established (Jones and Powell, 1970; Barbas and Mesulam, 1985; Barbas, 1986; Goldman-Rakic, 1988; Petrides and Pandya, 1988; Seltzer and Pandya, 1989; Hof *et al.*, 1995; Rempel-Clower and Barbas, 2000), and as mentioned above, many studies have documented the existence of age-related alterations in pyramidal neurons. However, the morphologic integrity of neurons providing identified corticocortical circuits has not been investigated with respect to putative age-related changes. The purpose of the present study is to assess in macaque monkeys the effect of aging on the dendritic integrity of a distinct subpopulation of pyramidal neurons furnishing a projection directly linked to cognitive processing, from the superior temporal cortex to the dorsolateral prefrontal area 46.

## Materials and Methods

### Animals and Surgical Procedures

Eleven monkeys, consisting of three adult male and two adult female long-tailed macaque monkeys (*Macaca fascicularis*, 10–12 years old), one adult male rhesus monkey (*Macaca mulatta*, 12 years old), and two aged male and three aged female rhesus monkeys (24–25 years old), were used in this study. Body size was 6–10 kg in the young group and 4.5–10 kg in the aged group. The range in weight in the aged group was

due mostly to the accumulation of body fat in one animal. The youngest male weighed 6 kg and the oldest female weighed 4.5 kg. The aged animals were all obtained from a single source (Bioqual Inc., Rockville, MD). They were born and raised in captivity and housed in cages for most of their lives. All of the aged monkeys included in the present analysis were retired breeders and none had been involved in any pharmacological or invasive studies. Monthly serological tests, annual physical exams and necropsy analyses did not reveal any factor that may have influenced the findings obtained in this study. Of note, potential effects of estrogen levels can be ruled out in the old females, since both groups included males and females. Also, all of the old females were still cycling at the time of the experiment. Some materials from these animals were used in previous studies of the morphology of corticocortical circuits (Duan *et al.*, 2002; Hof *et al.*, 2002). Additional materials were available from three young male rhesus monkeys (8–9 years old), two young (14 years old) and two aged (21 years old) female bonnet macaques (*Macaca radiata*), and one 27 years old female Moor's macaque (*Macaca maura*), from unrelated experiments that used a similar approach to the present study, and from three elderly humans free of neurologic or psychiatric disorders (75–82 years old). All experimental protocols were conducted according to National Institutes of Health (NIH) guidelines for animal research and were approved by the Institutional Animal Care and Use Committee (IACUC) at Mount Sinai School of Medicine. The control human specimens were acquired through the human brain bank of the Mount Sinai Alzheimer's Disease Research Center.

The animals were tranquilized with ketamine hydrochloride (25–25 mg/kg i.m.), intubated, and maintained under isoflurane general anesthesia and strict sterile surgical conditions (Hof *et al.*, 1995; Nimchinsky *et al.*, 1996; Duan *et al.*, 2002). They were placed for surgery in a custom-designed large animal head holder (David Kopf Instruments, Tujunga, CA) and a craniotomy was performed over the cortical site. The animals received injections of the retrograde tracer Fast Blue (FB) in ventral area 46 (Fig. 1). An aqueous solution of FB (4%; Sigma, St Louis, MO) was injected into the left hemisphere using a 5  $\mu$ l Hamilton microsyringe with a 24-gauge needle. In each animal, 9–12 300–400 nl injections were placed at depths from 0.6 to 1.2 mm below the pial surface. Following surgery, a survival time of 21 days was set to allow for optimal retrograde transport. The animals were then deeply anesthetized with ketamine hydrochloride (25 mg/kg) and pentobarbital sodium (20–35 mg/kg i.v.), intubated and mechanically ventilated. The chest was opened to expose the heart, and 1.5 ml of 0.1% sodium nitrite was injected into the left ventricle. The descending aorta was clamped and the monkeys were perfused transcidentally with cold 1% paraformaldehyde in phosphate-buffered saline (PBS) for 1 min, and then for 12 min with cold 4% paraformaldehyde and 0.125% glutaraldehyde in PBS. The bonnet and Moor's macaque samples were derived from animals which underwent similar procedures in the context of other projects. The human specimens were obtained at autopsy within 8 h of death and were immediately

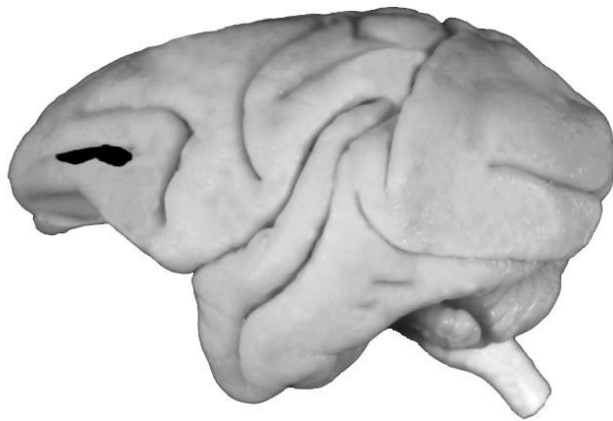


**Figure 1.** Surface rendering of the lateral view of a macaque monkey (*Macaca fascicularis*) brain showing the maximal extension of the intracortical FB injections (gray area) obtained from series of Nissl-stained sections in area 46 of the animals included in this study.

fixed by immersion in 4% paraformaldehyde. Small tissue blocks from the superior frontal cortex and superior temporal cortex were dissected out within 24 h of fixation and processed for intracellular injections as described below.

#### Tissue Preparation

Following perfusion, the brain was removed from the skull and 4–5 mm thick slabs of tissue were prepared from the prefrontal and temporal cortices. These tissues were blocked in a plane perpendicular to the principal sulcus in the prefrontal cortex or to the superior temporal sulcus in the temporal cortex. The blocks containing the injection sites were prepared to reconstruct the injection sites and verify that no injection penetrated the white matter. They were postfixed for 6 h in the same fixative, sectioned at 40  $\mu$ m on a Vibratome and stained with cresyl violet. One block was taken from the cortex located in the fundus of the superior temporal sulcus, corresponding to areas TPOr, IPa and TEa (de Lima *et al.*, 1990; Cusick *et al.*, 1995). This block was used for intracellular injection. Based on previous studies, FB-retrogradely labeled neurons in this temporal region form a strong association corticocortical projection to area 46 (Jones and Powell, 1970; Barbas and Mesulam, 1985; Barbas, 1986; Goldman-Rakic, 1988; Petrides and Pandya, 1988; Seltzer and Pandya, 1989; de Lima *et al.*, 1990; Hof *et al.*, 1995; Rempel-Clower and Barbas, 2000; Duan *et al.*, 2002). This block was postfixed for 2 h in the same fixative. Then, it was placed into PBS and cut at 400  $\mu$ m on a Vibratome in a semi-coronal plane that was orthogonal to the main axis of the superior temporal sulcus.

#### Intracellular Injections

For intracellular injection, the sections were mounted on nitrocellulose filter paper and immersed in PBS. Retrogradely labeled pyramidal cells located in the supragranular layers were identified under epifluorescence with a UV filter, impaled with sharp micropipettes, and loaded with 5% Lucifer Yellow (LY; Molecular Probes, Eugene, OR) in dH<sub>2</sub>O under a DC current of 3–8 nA for 10–12 min, or until the dye had filled distal processes and no further loading was observed (de Lima *et al.*, 1990; Nimchinsky *et al.*, 1996; Duan *et al.*, 2002). Generally, four to six FB-retrogradely labeled neurons were injected per slice, and such injections were placed far enough apart to avoid overlapping of the dendritic trees (Fig. 2A–C). After neuronal labeling, sections were fixed again in 4% paraformaldehyde and 0.125% glutaraldehyde in PBS for 4 h at 4°C, washed and stored in PBS. In order to be included for three-dimensional reconstruction, filled neurons had to satisfy three criteria: (i) they had to be located in layer III [accurate determination of cortical layers was performed on the fixed slice after counterstaining selected sections with 4,6-diamidino-2-phenylindole (DAPI; Sigma), a fluorescent nucleic acid stain]; (ii) the dendritic tree of the pyramidal cell had to be filled completely, which was judged at high magnification by tracing higher order branches to abrupt, well defined tips (Nimchinsky *et al.*, 1996; Duan *et al.*, 2002); and (iii) the absence of adjacent cells filled by the same injection and a reasonable distance among individual neurons had to allow for unambiguous determination of the exact origin of every filled dendritic segment.

#### Three-dimensional Reconstructions

Sections containing selected LY-filled neurons were then coverslipped with PermaFluor as a mounting medium, and reconstructed using a computer-assisted morphometry system consisting of a Zeiss Axiophot photomicroscope equipped with a Zeiss MSP65 computer-controlled motorized stage, a Zeiss ZVS-47E video camera system, a Macintosh G3 computer, and custom-designed morphometry software NeuroZoom (Nimchinsky *et al.*, 1996, 2000; Hof *et al.*, 2000). This system allows for accurate mapping and tracing of the cells and their processes in three dimensions. Neurons were located using a Zeiss Fluor 10 $\times$  objective and drawn using a Zeiss Aplanachromat 100 $\times$  objective with a numerical aperture of 1.4. A live RGB image was ported to the computer screen and mapping was performed by moving the stage in 1  $\mu$ m steps through the z-axis along the length of each dendrite. Spines were plotted at the same time. Then, the section itself was drawn at 10 $\times$ . In this manner, the x, y and z coordinates of each dendritic segment and spine were recorded to enable later three-dimensional representation and rotation of the reconstructed neuron (Nimchinsky *et al.*, 1996). Up to six neurons were fully

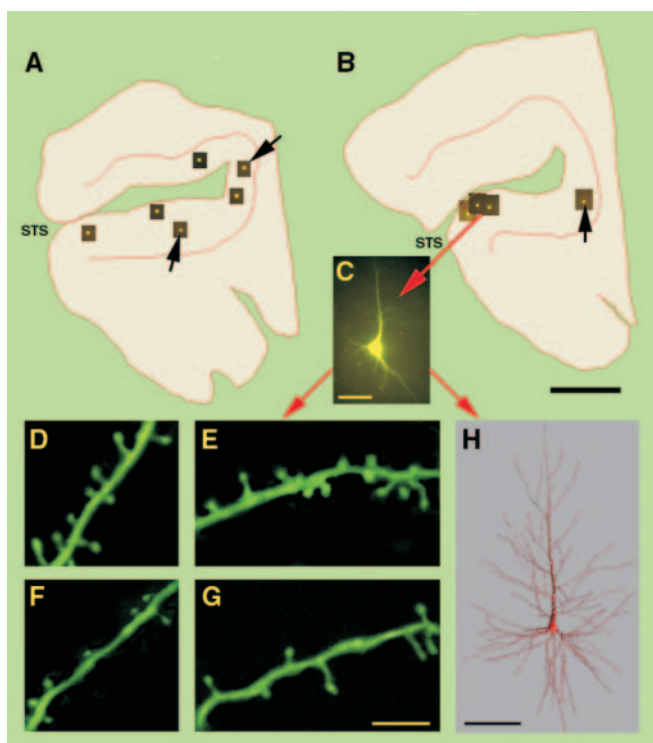


**Figure 2.** Flow chart of the labeling and analysis procedures. The FB-retrogradely labeled neurons are visualized in thick sections of the temporal cortex and their positions are mapped (A, B). The dark rectangles with a yellow square represent actual screen dumps of a labeled neurons in the context of the full-scale map of the section (scale bar = 2 mm for both maps; STS, superior temporal sulcus). The neurons indicated by black arrows were located in layer V and were not analyzed in the present study. An example of a LY-loaded neuron is shown in (C) under epifluorescence conditions and intermediate magnification (scale bar = 40  $\mu\text{m}$ ). Panels D–G show confocal laser scanning imaging of apical (D, F) and basal (E, G) dendritic segments in a young (D, E) and an aged (F, G) rhesus monkey. Note that the technique permits the recovery of fine morphologic details of spines and that there is a clear decrease in spine numbers in the segments from the old animal (scale bar on G = 8  $\mu\text{m}$ ). (H) shows a NeuroGL three-dimensional model of a LY-loaded neuron after reconstruction (scale bar = 100  $\mu\text{m}$ ).

reconstructed from each subject (for a total of 33 neurons in young animals and 19 neurons in old animals). Additional data on spine densities were obtained from neurons that were not fully filled, but only from cases where the branch order number of a given dendritic segment could be established unequivocally; typically these were neurons from which only the apical or the basal trees had been successfully loaded. Only data on spine densities were obtained from humans, and bonnet and Moor's macaque specimens, for comparison with results from the long-tailed and rhesus macaques on which this study is based. Dendritic segments from a subgroup of neurons were imaged on a confocal laser scanning microscope (Zeiss LSM 410; Zeiss Oberkochen, Germany) to ascertain the quality of cell loading (Figs 2D–G, 8A–D). Lucifer Yellow was visualized with an ArKr 488/568 laser and a 515–565 bandpass emission filter were used. Neurons were located using a Zeiss NeoFluar 16 $\times$  objective and observed using a Zeiss Apochromat 100 $\times$  objective with a numerical aperture of 1.4. To resolve spine morphology adequately a zoom factor of 8 was applied.

The NeuroZoom datasets were then exported to generate three-dimensional renderings of the traced neurons using NeuroGL, a self-contained, compact, and fast application to visualize structural details of neurons, including branching patterns, spine location and spine density, at a range of scales and in an interactive three-dimensional environment (Henry *et al.*, 2001; Rodriguez *et al.*, 2003) (see also <http://www.mssm.edu/cnic> for details).

### Morphological Analysis

Dendrograms showing the branching pattern of each dendritic tree were prepared for each reconstructed neuron using NeuroZoom. Branch orders were evaluated in an adapted centrifugal fashion with minor modifications for the apical dendrites and a centrifugal fashion for the basal dendrites (Uylings *et al.*, 1986). Dendrites arising from the cell body were considered as first-order segments until they bifurcated symmetrically into second-order segments; dendritic branches arising from the first-order segments were considered as second-order segments until they bifurcated symmetrically into third-order segments, and so on. In cases of asymmetric branching, the offspring dendrite could generally be recognized by a qualitatively thinner diameter and would be classified as a next-order branch whereas the parent dendrite would retain its order level past the branching point. These criteria were consistently applied throughout the study. For analytical purposes, data on apical and basal dendrites were kept separate. Using the three-dimensional capabilities of the software, we quantified the following parameters for each reconstructed neuron: (i) total dendritic length, representing the summed length of dendritic segments; (ii) dendritic segment counts, representing the total number of dendritic segments; (iii) total dendritic spine number, representing the sum of all spines on dendritic segments; (iv) dendritic spine density, representing the average number of spines per  $\mu\text{m}$  of dendritic length. To localize age-related changes within the dendritic arbors, branch order-level analyses were performed for the dendritic length, dendritic segment counts, dendritic spine numbers and spine density per branch order using SpineCT, a custom Java software. The dendritic branching patterns were also analyzed using Sholl's method of regularly spaced concentric circles centered on the neuronal soma (Sholl, 1953). The number of dendritic intersections crossing each 20  $\mu\text{m}$ -radius circle progressively more distal from the soma was counted. For each of these parameters, an average was calculated for each animal. Means for the young and aged groups were then obtained from these individual values. It must be kept in mind that a certain degree of three-dimensional tissue shrinkage occurred during processing due to aldehyde fixation. We did not introduce a correction factor in the present study. As such, all quantitative data represent post-shrinkage measurements and thus are likely to underestimate the true size of these neurons.

Statistical analysis was performed using analysis of variance to assess possible differences in the various morphometric parameters among cases within each group. As the variance between animals in each age group was small and the variances of each subject did not differ significantly for each of the measured parameters, data were expressed as means from all animals from both age groups. Age-related differences in these variables across the total, apical and basal dendritic domains were compared using *post hoc t*-tests, and using Tukey tests for groups with unequal numbers when comparing means for each branch order. Finally, the data from the Sholl analyses were also expressed as cumulative frequencies and statistical differences between the two groups were assessed using the Kolmogorov–Smirnov test. Differences were considered statistically significant at  $P < 0.05$ .

## Results

### Morphology of LY-filled Neurons

In all of the 11 monkeys, injections of FB in the ventral part of area 46 resulted in large numbers of retrogradely labeled neurons in the ipsilateral cortex lining the dorsal and ventral aspects of the superior temporal sulcus. These long projection neurons formed two clearly defined bands, corresponding to layers III and V–VI, as demonstrated in previous studies of macaque monkeys (Jones and Powell, 1970; Barbas and Mesulam, 1985; Barbas, 1986; Goldman-Rakic, 1988; Petrides and Pandya, 1988; Seltzer and Pandya, 1989; Hof *et al.*, 1995; Rempel-Clower and Barbas, 2000; Duan *et al.*, 2002; Hof *et al.*, 2002).

More than 15 retrogradely labeled neurons were adequately filled with LY in each animal. Up to six neurons in layer III were fully reconstructed in each monkey. In total, 27 fully reconstructed neurons were analyzed from the six young monkeys and 19 from the five old monkeys. All of the filled neurons used for

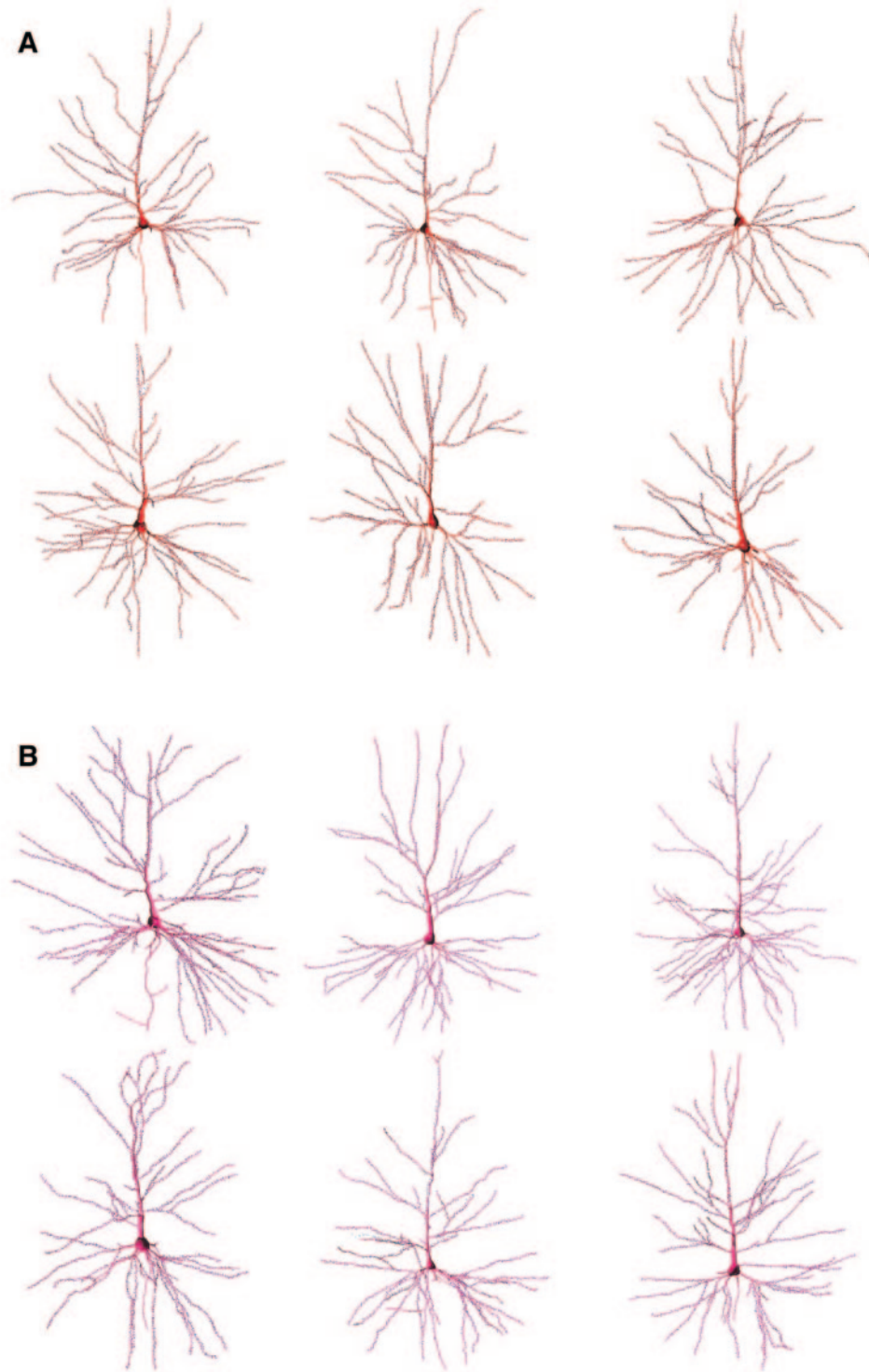


**Figure 3.** Representative examples of three-dimensional reconstructions of corticocortically projecting pyramidal cells with spines plotted on the dendritic trees. These three-dimensional reconstructions of neurons were obtained using NeuroGL and are rendered with variable scaling and degrees of rotation about their principal axis to depict the extent of their basal and apical dendritic arborization. Neurons in (A) are from young animals and neurons in (B) are from aged animals. Note that at this level of resolution, the general morphology and complexity of neurons shown in (A) appear similar to the neurons in (B).

reconstructions exhibited a typical pyramidal morphology (i.e. they had a triangular cell body, a prominent apical dendrite oriented toward the pia and at least two basal dendrites). Examples of reconstructed neurons forming long projections

from the superior temporal cortex to ipsilateral area 46 in both young and old monkeys are shown in Figure 3. All of these neurons exhibited extensive dendritic branching with large numbers of spines (Figs 2D–G, 3). Verification of the quality

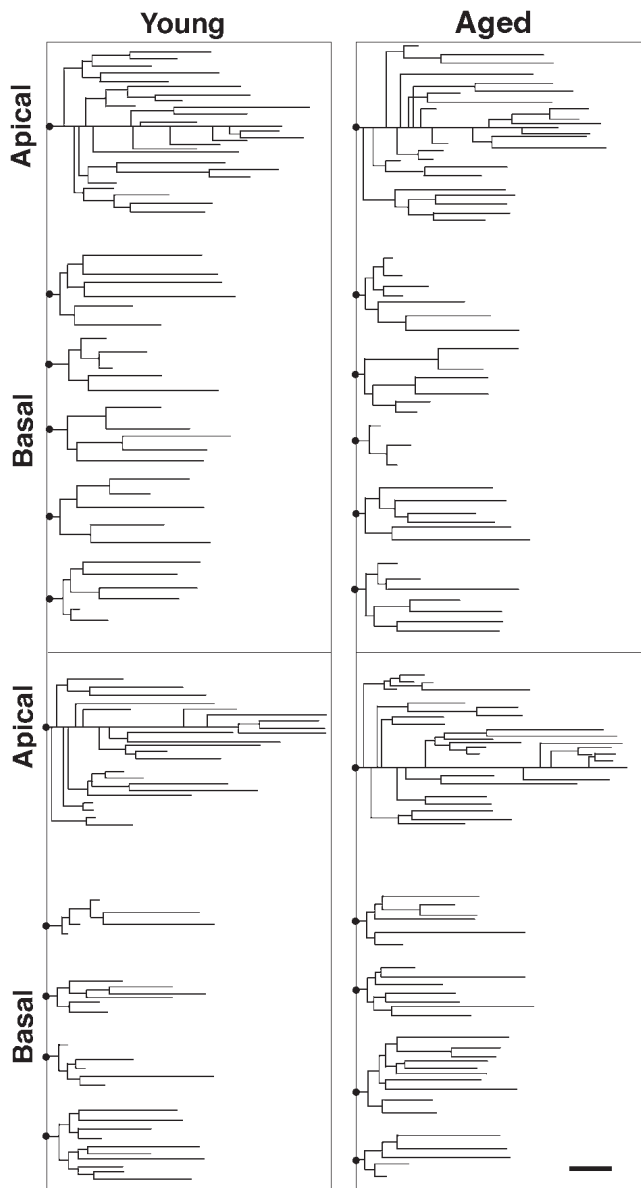


**Figure 4.** Representative dendrograms of apical and basal dendritic trees of neurons from young and aged animals. The soma of these neurons is located to the left of the dendrites (noted by a black dot on the dendrograms). These dendrograms show the general branching patterns of the dendritic trees and are scaled in terms of length and complexity. The overall dendritic extent and complexity of neurons from young and aged animals are not different. Scale bar = 50  $\mu\text{m}$ .

of cell loading on a confocal laser scanning microscope showed excellent recovery of dendritic and spine morphology and helped confirming the quantitative analyses (Fig. 2D–G).

#### **Dendrograms and Sholl Analysis of Dendritic Arbors**

Dendrograms of representative neurons forming long projections from young and aged animals are shown in Figure 4. These dendrograms demonstrate the overall branching patterns of the dendritic trees and are scaled in terms of length and complexity. This analysis revealed that there were no qualitative differences between the two groups of animals with respect to dendritic length and complexity, in both the apical and basal dendrites (Fig. 4).

The complexity of apical and basal dendritic trees of these

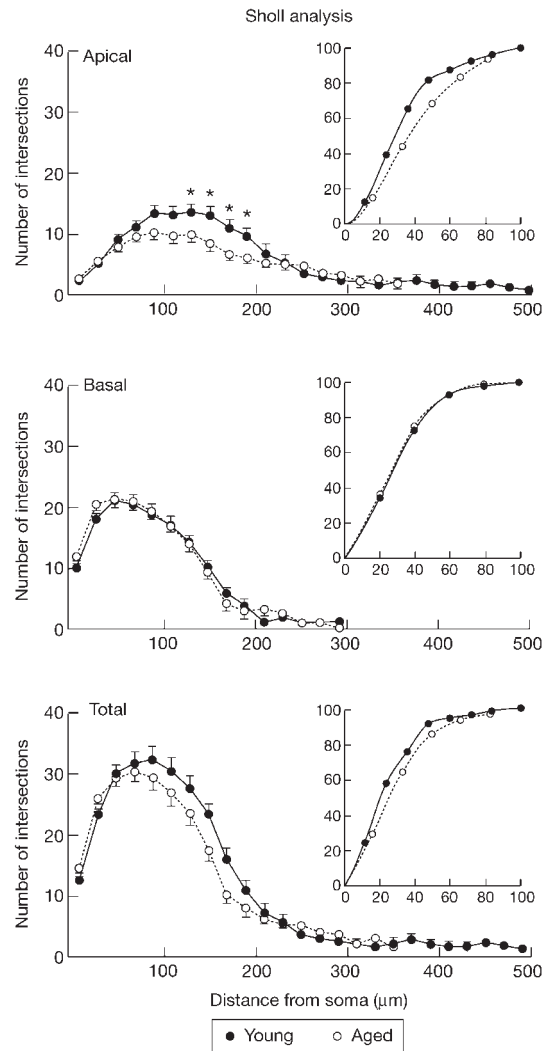


**Figure 5.** Sholl analysis of long projection neurons from young (black lines) and old (dotted lines) macaque monkeys. Asterisks indicate statistically significant differences across the dendritic trees (\* $P < 0.05$ ; \*\* $P < 0.01$ ). Values represent means  $\pm$  SEM. Cumulative frequency plots (insets) of the distribution of Sholl intersections along the dendritic trees revealed statistically significant differences only for the apical dendrites of neurons between the young and aged animals. The abscissa and ordinate on the insets represent percent of total distance from the soma, and numbers of intersections, respectively (for clarity some of the data points were omitted).

pyramidal neurons was further assessed using Sholl analysis (Fig. 5). Significant age-related decreases in the numbers of intersections between the dendrites and the Sholl circles occurred only between 140  $\mu\text{m}$  and 180  $\mu\text{m}$  from the neuronal somata (Fig. 5;  $P < 0.05$ , Tukey test) in the apical dendrites. There were no differences in the numbers of intersections between young and aged groups at any distance from the soma for the basal dendrites. The difference between the two age groups in the distribution of cumulative frequencies of the numbers of intersections along the dendritic arbors was statistically significant only for the apical dendrites (Fig. 5;  $P < 0.05$ , Kolmogorov–Smirnov test).

#### **Quantitative Analyses of Dendritic Segments and Spines Densities**

The average total dendritic lengths of the apical and basal dendrites in the aged monkeys were  $1923.9 \pm 151.0 \mu\text{m}$  and

**Table 1**

Morphometric dendritic measurements of cortical neurons from young and aged animals

Parameter	Young	Aged	% Difference	<i>P</i> value
<i>Total dendritic length</i>				
Total	5430.9 ± 364.4 <i>5821 (5612.3)</i>	4748.3 ± 238.3	-12.8	NS
Apical	2541.1 ± 264.5 <i>2754 (2788.4)</i>	1923.9 ± 151.0	-24.3	NS
Basal	2889.8 ± 148.3 <i>3066 (2823.9)</i>	2824.4 ± 160.9	-2.3	NS
<i>Total dendritic segments</i>				
Total	86.6 ± 4.4 <i>88 (89.0)</i>	81.9 ± 7.5	-5.4	NS
Apical	36.4 ± 3.0 <i>31 (33.2)</i>	30.0 ± 3.7	-17.6	NS
Basal	50.1 ± 2.4 <i>54 (55.8)</i>	51.8 ± 4.1	+3.4	NS
<i>Total spine number</i>				
Total	2845.0 ± 192.8 <i>3376 (3432.5)</i>	1869.7 ± 67.0	-34.3	<0.01
Apical	1378.4 ± 156.0 <i>1652 (1756.7)</i>	791.3 ± 51.7	-42.6	<0.01
Basal	1466.6 ± 65.9 <i>1686 (1666.1)</i>	1078.4 ± 70.5	-26.5	<0.01
<i>Spine density</i>				
Total	0.53 ± 0.02 <i>0.58 (0.61)</i>	0.39 ± 0.02	-26.4	<0.01
Apical	0.54 ± 0.02 <i>0.60 (0.63)</i>	0.41 ± 0.02	-24.1	<0.01
Basal	0.51 ± 0.02 <i>0.55 (0.59)</i>	0.38 ± 0.03	-25.4	<0.01

Dendritic lengths are in  $\mu\text{m}$  and spine densities are expressed per  $\mu\text{m}$  of dendrite. Data represent means  $\pm$  SEM. The values in italics in the column representing young animals are from the one young rhesus monkey and the values in parentheses are the means from the six superior temporal cortex pyramidal neurons that were retrieved and fully reconstructed from three additional young rhesus monkeys. These are within the distribution range of the data and there is no indication of a *mulatta* vs *fascicularis* species differences (see Fig. 8 for additional comparative data on spine densities among macaque species and humans). Note that the differences between cortical neurons from young and aged animals are about spine numbers and spine density but that dendritic length and segment numbers do not differ between the two groups of investigated neurons

NS, non-statistically significant.

2824.4  $\pm$  160.9  $\mu\text{m}$ , respectively (means  $\pm$  SEM). There were no significant differences between these values and those from the young animals (2541.1  $\pm$  264.5  $\mu\text{m}$  for apical dendrites and 2889.8  $\pm$  148.3  $\mu\text{m}$  for basal dendrites). The number of dendritic segments for the apical (aged = 30.0  $\pm$  3.7, young = 36.4  $\pm$  3.0) and basal (aged = 51.8  $\pm$  4.1, young = 50.1  $\pm$  2.4) dendrites did not change significantly during aging in these long projection neurons. In contrast, there was a marked age-related decrease in dendritic spine numbers and densities for both the apical and basal dendrites in all of the reconstructed neurons (Table 1; Fig. 6). Dendritic spine numbers decreased by ~43% and 27% for the apical and basal dendrites, respectively, in aged monkeys ( $P < 0.01$  in both cases, *t*-test). Spine densities decreased by ~25% for both the apical and basal dendrites in the aged animals compared with the young ones ( $P < 0.01$  in both cases, *t*-test). The changes in spine densities for the apical and basal dendrites of these long projection neurons are also shown qualitatively in Figures 2D-G, 7 and 8A-H.

It should be noted that only one of the young animals, but all of the old ones, were rhesus monkeys. This raises the possibility that the observed age-related changes in these parameters are due to species differences, if the long-tailed macaques were to have larger neurons or more spines than the rhesus monkeys. This is however not likely as the values from the one young rhesus monkey were in fact consistently high compared with those

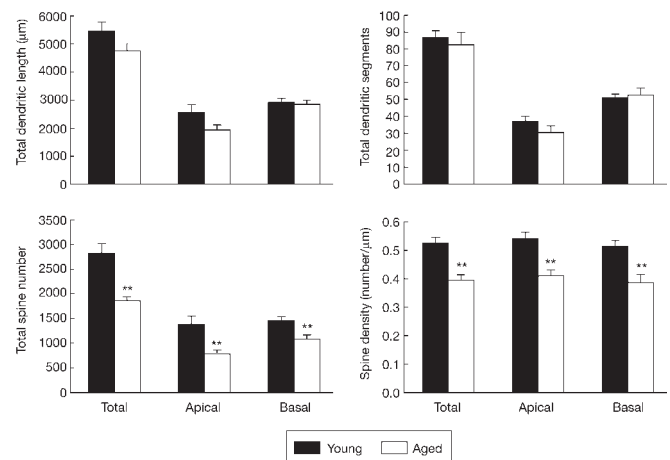


**Figure 6.** Histograms showing the quantitative data (means  $\pm$  SEM) from the reconstructed projection neurons in the 11 young and aged macaque monkeys used in this study. Statistically significant differences are indicated by asterisks (\*\* $P < 0.01$ ).

recorded in the young long-tailed macaques, for all measurements (see Table 1, *italicized* values). As further support to this fact is that all parameters retrieved from six fully reconstructed superior temporal cortex pyramidal neurons in three young rhesus macaques used in unrelated experiments with a similar design were not different from those in the young rhesus and long-tailed macaques originally included in this study (Table 1 and Figs 5-10), and did not modify our conclusions. Also, spine densities from old and young bonnet macaques and from one very old Moor's macaque, were well within the range of our observations in long-tailed and rhesus macaques, arguing strongly against differences in spine densities among macaque species (Fig. 8). Furthermore, data from all of the young and old animals of the four macaque species considered in this study were comparable to results obtained from Patas monkeys (Page *et al.*, 2002) (Fig. 8). Interestingly, humans had considerably higher spine densities (Fig. 8), a fact also noted by Elston and colleagues (Elston *et al.*, 2001; Elston and DeFelipe, 2002).

### Branch Order Analysis

Figure 9 shows the average dendritic branch length and numbers of dendritic segments per branch order. Age-related decreases in dendritic length and segment numbers were significant only at the second branch order for the apical dendrites. No differences in dendritic length and segment numbers were observed at any branch order for the basal dendrites between the two age groups. Likewise, the highest branch order attained by each age group was not different (with six orders for the apical dendrites and seven for the basal dendrites, respectively).

The age-related spine changes were further analyzed by measuring the average spine numbers and spine density per branch order (Fig. 10). On apical dendrites, dendritic spine numbers decreased significantly in the first three orders (Fig. 10;  $P < 0.05$ -0.01, Tukey test), while the spine density decreased more uniformly across the different branch orders in the aged group (Fig. 10;  $P < 0.05$ -0.01, Tukey test). On basal dendrites, decreases in spine numbers (Fig. 10;  $P < 0.05$ , Tukey test) and spine density (Fig. 10;  $P < 0.01$ , Tukey test) were observed only in more distal branch orders (i.e. on branch orders 3 and 6). The data from the isolated neurons obtained from the three additional young rhesus monkeys did not alter these results.

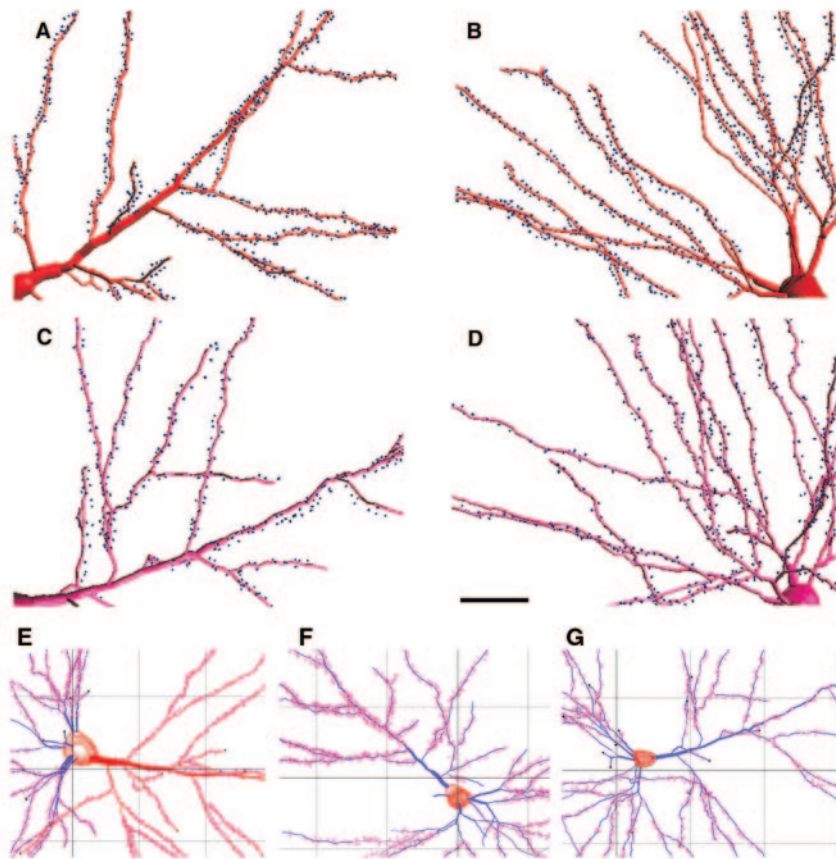


**Figure 7.** Examples of apical and basal dendritic segments with spines plotted onto them from young and aged animals showing age-related differences in spine density. These dendritic segments were obtained using NeuroGL and are rendered at the same scaling. (A) and (B) are from the apical and basal dendritic trees, respectively, of a neuron from a young animal. (C) and (D) are from the apical and basal dendritic trees, respectively, of a neuron from an old animal. (E) and (F) are flattened renditions of parts of pyramidal neurons traced using NeuroZoom from a young long-tailed (E) and a young rhesus macaques (F). There are no differences in spine densities between the two species. (G) shows a similar map from an old rhesus monkey. There are visible decreases in spine numbers on the apical and basal dendrites in the aged animals (C, D, G). Compare with Figure 2D–G. Scale bar (on D) = 20  $\mu\text{m}$ ; the size of the grid in (E–G) is 50  $\times$  50  $\mu\text{m}$ .

## Discussion

The neurons of origin of long association corticocortical pathways differ neurochemically and morphologically from those providing short projections (Hof *et al.*, 1995, 2002; Duan *et al.*, 2002). Neocortical neurons furnishing long corticocortical projections have longer, more complex dendritic arbors and more spines than those providing short projections (Duan *et al.*, 2002), rendering them capable of performing more complex cortical functions such as cognition (Elston, 2000; Elston *et al.*, 2001; Jacobs *et al.*, 2001; Elston and DeFelipe, 2002). Moreover, neurons forming long corticocortical projections are preferentially enriched in neurofilament protein (Hof *et al.*, 1995, 2002), and have been found to be highly vulnerable to the degenerative process in Alzheimer's disease, and thus, their disruption may lead to a complex syndrome of cortical disconnection that is reflected in the dementing symptomatology observed in Alzheimer's disease patients (Hof *et al.*, 1990; Morrison and Hof, 1997). These data suggest that the neurons providing long corticocortical pathways have unique phenotypes and are critical for the high-level cognitive function of the cerebral cortex. Importantly, the projection investigated in the present study is considered to play a critical role in cognition (Goldman-Rakic, 1988) and degenerates extensively in humans with Alzheimer's disease (Hof *et al.*, 1990; Morrison and Hof, 1997).

Although studies have investigated dendritic changes during normal aging in human and nonhuman primates, the impact of aging on the extent and integrity of the dendritic tree has not yet been quantified in a subset of projection neurons forming an identified corticocortical projection. We used a method of *in vivo* retrograde tract-tracing in combination with cell loading in fixed slices and three-dimensional neuronal reconstructions (de Lima *et al.*, 1990; Nimchinsky *et al.*, 1996; Duan *et al.*, 2002; Page *et al.*, 2002). This method yields high quality labeling of dendritic structures (dendrites and dendritic spines) of the targeted neurons, which is critical for a quantitative analysis of dendritic extent and spine numbers on the neurons providing an identified projection. As discussed in a previous study (Duan *et al.*, 2002), however, some practical problems do exist at present. For example, sectioning tissue at 400  $\mu\text{m}$  will result in cut dendritic segments. Therefore, measurements in this study represent estimates rather than absolute values because the full dendritic extent may not be assessed in all cases with certainty. Also, difficulties in estimating three-dimensional shrinkage due to tissue processing with any accuracy results in datasets that represent underestimates of the actual size of these neurons, and may induce some degree of spatial distortion (Trommald *et al.*, 1995). Furthermore, with respect to spine measurements, spines that lie either on the backside of the dendrites or spines that are pointing directly up at the viewer cannot be seen

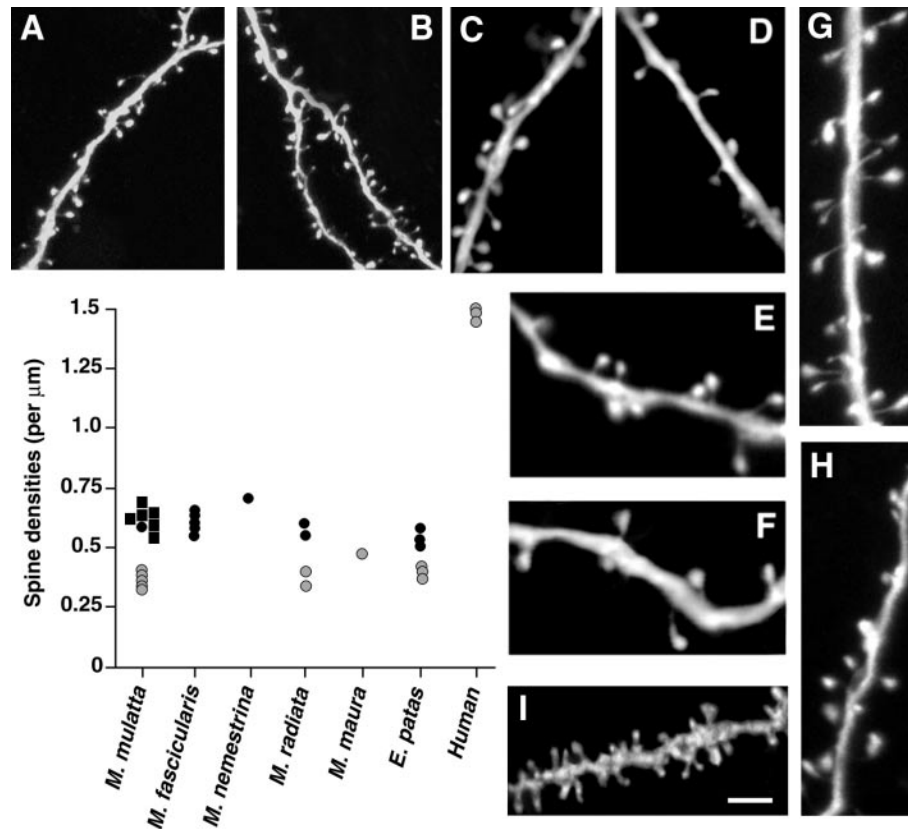


**Figure 8.** Spine densities on neocortical pyramidal neurons from the 11 animals on which the present study is based (*M. mulatta* and *M. fascicularis* in the graph), compared with available data from four bonnet macaques (*M. radiata*), one Moor's macaque (*M. maura*), six patas monkeys (*E. patas*) and three humans. The data from *E. patas* were reported in Page *et al.* (Page *et al.*, 2002), and those from *M. radiata*, *M. maura* and from humans are unpublished observations. An additional data point from the pig-tailed macaque (*M. nemestrina*) was obtained from Boothe *et al.* (Boothe *et al.*, 1979) for further comparison. In the graph, aged specimens are designated by gray dots and young adult specimens by black dots. Additional average values from a limited number of neurons ( $n = 6$ ) retrieved from three young *M. mulatta* are indicated by black squares. Data on the graph are derived from the entire dendritic arbor of neurons that were identified and analyzed using as described in the Materials and methods section (except for *M. nemestrina*). Panels A–I show representative confocal laser scanning microscopy examples of spine morphology and density in a young adult *M. mulatta* (A) and a young adult *M. fascicularis* (B), an adult (C) and old (D) *M. radiata*, a young (E) and old (F) *E. patas*, the old *M. maura* (G, H), and an elderly normal human (I). There is a striking consistency in spine densities in old and in young animals across these macaque species. Note the much higher spine densities on the human dendrite compared with all of the macaque specimens. The scale bar (on I) = 6  $\mu\text{m}$  (A, B, I), 3  $\mu\text{m}$  (C, D), and 2  $\mu\text{m}$  (E–H).

reliably with standard light microscopy or with epifluorescence (Feldman and Peters, 1979; Trommald *et al.*, 1995). Thus, measurements of spine numbers and spine density with the light microscope will necessarily underestimate the total number of spines. Such undercounting errors in apparent spine numbers may be as high as 30–50% based on Golgi impregnations of rat neocortical neurons (Feldman and Peters, 1979), but there is not direct ways to compare Golgi-impregnated to LY-loaded materials in terms of their respective (and most probably equally variable) success at labeling spines. Indeed, more accurate estimates of the true total population of spines can be achieved by high resolution three-dimensional reconstruction of neurons at high magnification using confocal microscopy (Trommald *et al.*, 1995; Rodriguez *et al.*, 2003); see also Fig. 2D–G. This process is however extremely time-consuming when analyzing large neocortical neurons, and generates very large datasets requiring deconvolution (Rodriguez *et al.*, 2003). Whereas this approach was well beyond the scope of the present study, these methodological limitations affected all neurons in our sample equally and therefore had no direct effect on the observed differences in spine densities and other parameters between the two age groups. It should be noted, however, that the distribution, numbers and densities of spines on basal trees reported

in this study are consistent with the results reported by Elston and colleagues using a slightly different approach (Elston and Rosa, 2000; Elston *et al.*, 2001; Elston and DeFelipe, 2002).

We observed statistically significant and consistent decreases in the total numbers of spines and spine density on both the apical and basal dendrites of layer III pyramidal neurons forming long corticocortical projections from the temporal cortex to prefrontal area 46 in old animals compared with young animals. On the apical dendrites of aged animals, changes in spine numbers were observed mainly on the proximal dendrites (branch orders 1–3), but spine density decreased uniformly among the different branch orders. On the basal dendrites of aged animals, the spine numbers and spine densities decreased preferentially on the distal branch orders (orders 3–6). Although there was a trend toward shorter total dendritic lengths (~24%) and fewer total segments in the apical trees of old monkeys, these trends failed to reach statistical significance, and were absent in the basal trees. Age-related decreases in dendritic length and segment numbers were observed only at the second branch order for the apical dendrites. Sholl analyses revealed that age-related dendritic regressive changes are restricted to a very limited portion of the apical dendrites. This difference, and the fact that spine loss varies depending on the branch order on

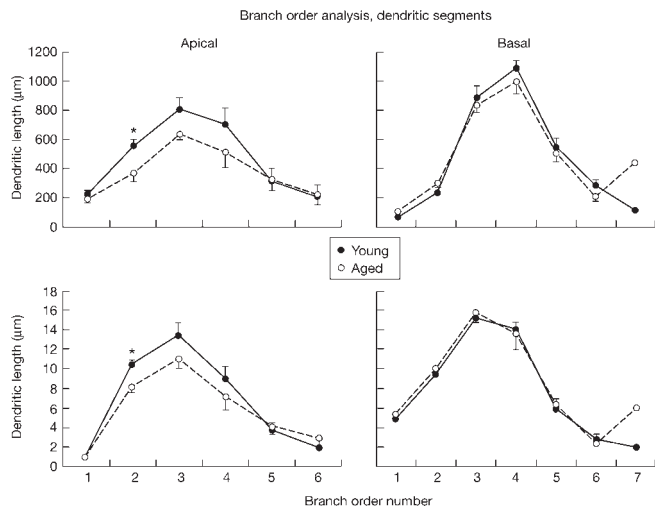


**Figure 9.** Branch order analyses of average dendritic length and numbers of dendritic segments at each branch order for the apical and basal dendrites in young and aged animals. Statistically significant differences are indicated by asterisks ( $*P < 0.05$ ). Values represent means  $\pm$  SEM. Age-related decreases in dendritic length and segment numbers were observed only at the second branch order for the apical dendrites.

apical and basal trees, may reflect the demise of specific cortical inputs targeting preferentially these portions of the dendritic tree. This supports the notion that neocortical pyramidal neurons display a range of spine distribution that is related to their connectivity patterns (Pucak *et al.*, 1996; Melchitzky *et al.*, 1998; Duan *et al.*, 2002; Soloway *et al.*, 2002), and suggests that only a restricted number of corticocortical projections are selectively affected by the aging process. This will require confirmation using anterograde labeling of projections combined with electron microscopy analyses in aged monkeys.

Regressive dendritic changes in cortical pyramidal neurons during aging have been reported in the prefrontal cortex of human (Scheibel *et al.*, 1975; Jacobs *et al.*, 1997; de Brabander *et al.*, 1998) and nonhuman primates (Cupp and Uemura, 1980; Peters *et al.*, 1998b), in the human motor cortex (Nakamura *et al.*, 1985) and superior temporal gyrus (Jacobs and Scheibel, 1993; Anderson and Rutledge, 1996). In contrast, dendritic growth has been reported in layer II neurons of the human parahippocampal gyrus (Buell and Coleman, 1979, 1981). These apparently conflicting results on age-related alterations in cortical pyramidal dendrites have been explained by the possibility that dendritic extent in normal aging exhibits regional specificity (Coleman and Flood, 1987; Jacobs and Scheibel, 1993; Jacobs *et al.*, 1997). More recently, de Brabander *et al.* (de Brabander *et al.*, 1998) have reported a layer-specific dendritic regression of cortical pyramidal neurons during aging in a human study. De Brabander and colleagues examined the basal dendritic branching pattern in the human prefrontal cortex from eight subjects ranging in age from 49 to 90 years, all without neurological or psychiatric disorders, and demonstrated decreases in total dendritic length, total numbers of dendritic segments, and terminal dendritic length in the basal dendrites of layer V pyramidal neurons in the prefrontal cortex with increasing age, whereas layer III neurons did not show any age-related changes on their basal dendrites.

The present study extends these findings by showing that the dendritic morphology of cortical pyramidal neurons forming long corticocortical projections remains generally stable in aged

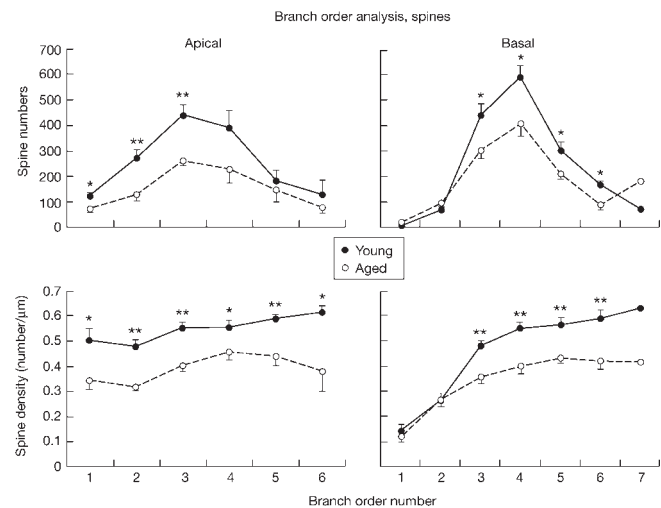


**Figure 10.** Branch order analyses for the average spine number and spine densities at each branch order for the apical and basal dendrites in young and aged animals. Statistically significant differences are indicated by asterisks ( $*P < 0.05$ ;  $**P < 0.01$ ). Values represent means  $\pm$  SEM.

monkeys but that dendritic arbors exhibit local regressive changes. The functional repercussions of these changes remain unclear. However, it is possible that age-related local changes in the dendritic length, numbers of segments and branching patterns may alter the neuron's response to synaptic input in a given layer or sublayer even though the general dendritic morphology is not significantly modified. Significantly, the present study analyzed the dendritic spine numbers and densities across the entire dendritic trees of these layer III pyramidal neurons. In sharp contrast with the overall stability of the dendritic morphology during aging,  $\sim 43\%$  and  $27\%$  loss of spines were found in the old animals compared with the young animals in the apical and basal dendrites, respectively, and  $\sim 25\%$  decrease in spine density was found in both the apical and basal dendrites. These findings are consistent with previous investigations of broader populations of pyramidal cells (Uemura, 1980; Anderson and Rutledge, 1996; Jacobs *et al.*, 1997; Peters *et al.*, 1998b; Page *et al.*, 2002). A few quantitative Golgi studies have examined the effect of age on the spine numbers or spine densities of cortical pyramidal neurons in the human brain. Anderson and Rutledge (Anderson and Rutledge, 1996) quantified spine numbers on the basal dendrites of supragranular pyramidal cells in the posterior superior temporal gyrus and noted a significant decline in spine numbers between 21 and 71 years of age. Jacobs and colleagues examined the total dendritic spine numbers, and dendritic spine densities on basal dendrites of supragranular pyramidal cells in prefrontal area 10 and occipital area 18 in materials obtained from 26 neurologically normal individuals 14–106 years old (Jacobs *et al.*, 1997). These authors reported a 46% decrease in spine numbers and spine density from the younger group ( $= 50$  years) to the older group ( $> 50$  years) in both areas. Similar results have been found in studies of non-human primates. In a Golgi study, Uemura (Uemura, 1980) reported a 29% decrease of spine density on the apical and basal dendrites of layers III and V pyramidal neurons in the prefrontal cortex of macaque monkeys 7–28 years old. In a more recent electron microscopy study, Peters *et al.* (Peters *et al.*, 1998b) noticed a 50% loss in spines on the apical dendritic tufts of pyramidal cells in layer I of area 46 of old monkeys (27–32 years of age) compared to young monkeys (6–9 years of age).

We recently reported a 35% loss of spines and ~20% decrease of spine density on the apical and basal dendrites of cortical pyramidal neurons forming long corticocortical projections in a study of old Patas monkeys [*Erythrocebus patas* (Page *et al.*, 2002)], a cercopithecine species related to macaques but phylogenetically closer to guenons. The fact that our quantitative findings appear consistent across genera within cercopithecine monkeys is also an argument against the occurrence of species-level differences within genus *Macaca*. This is further exemplified by the highly consistent densities of spines in both age groups observed among the four macaque species considered in the present analysis (see Fig. 8). It is worth noting that from a taxonomic point of view, the long-tailed and the rhesus macaque are the most closely related of these species belonging to the so-called '*fascicularis*' and '*mulatta*' species-groups, whereas the bonnet and the Moor's macaque are representative of more distantly related macaque groups [the '*sinica*' and '*Sulawesi*' species-groups, respectively (Fooden, 1976; Groves, 2001)]. The observed consistency in spine data and these taxonomic relationships among macaques make it highly unlikely in our view that species differences were responsible for the differences between age groups reported in the present study. A Golgi-based study of pig-tailed macaques (*Macaca nemestrina*) also found spine densities in layer III of the occipital cortex that are comparable to our observations (Boothe *et al.*, 1979). Moreover, estimates of spine numbers from neurons in the temporal neocortex of a much smaller-bodied callithricine, the common marmoset (*Callithrix jacchus*), and in the owl monkey (*Aotus trivirgatus*, a medium-bodied nocturnal ceboid), fall within the lower range of those in macaques (Elston *et al.*, 2001; Elston and DeFelipe, 2002; Elston, 2003), further supporting this point. Remarkably, human neocortical pyramidal neurons had higher spine densities than similar cells in other primate species, as previously reported (Elston *et al.*, 2001; Elston and DeFelipe, 2002). This is possibly related to the larger neuronal size as well as the higher cognitive abilities of our own species (Elston *et al.*, 2001; Benavides-Piccione *et al.*, 2002). Whereas spine numbers may reflect species-specific adaptive evolutionary events and may not be related to simple scaling laws (Harrison *et al.*, 2002), the fact that humans differ in this parameter deserves further attention. The issue of difference in spine densities among primate taxa will be ultimately better addressed in a sample including prosimians and great apes as well as common macaques.

Interestingly, Feldman and Dowd (Feldman and Dowd, 1975) reported a 24–40% loss of spines in aged rats, suggesting that spine loss may be a fairly consistent feature of brain aging in a number mammalian taxa. Because dendritic spines are the major postsynaptic sites of excitatory synapses on cortical pyramidal neurons (Horner, 1993; Harris and Kater, 1994; Nimchinsky *et al.*, 2002), changes in dendritic spine numbers may reflect a similar change in synaptic density. Indeed, a parallel reduction of synaptic density with senescence has been observed in quantitative electron microscopy studies (Uemura, 1980; Peters *et al.*, 1998b). In human prefrontal cortex, synapse densities were found to remain fairly constant in adults, but to show a progressive, significant decrease in individuals older than 74 years (Huttenlocher, 1979). Following a considerable decrease in synapse numbers during puberty, a continued, slight, yet statistically significant loss of synapses occurs in macaque monkey neocortex (Zecevic *et al.*, 1989; Bourgeois and Rakic, 1993; Bourgeois *et al.*, 1994). This synaptic loss is paralleled by a decrease in the number of dendritic spines in macaque monkeys suggesting continuing maturational changes throughout the life

span (Lund *et al.*, 1977; Boothe *et al.*, 1979; Elston and DeFelipe, 2002). Interestingly, the overall distribution of spines on dendritic segments remains unchanged during aging in spite of the observed decrease (Elston and DeFelipe, 2002) (present study). In this context, it is worth noting that the expression levels of AMPA ( $\alpha$ -amino-3-hydroxy-5-methyl-4-isoxazole propionic acid) and NMDA (*N*-methyl-D-aspartate) glutamate receptor subunit proteins GluR2 and NMDAR1 decreased significantly in many corticocortical projections in aged macaque and Patas monkeys (Hof *et al.*, 2002). NMDAR1 levels were also found to decrease specifically and consistently in the molecular layer of the dentate gyrus, specifically in the zone receiving the projections from the entorhinal cortex, in aged macaque monkeys without changes in other synaptic and dendritic markers (Gazzaley *et al.*, 1996). This change occurred in absence of neuronal loss in the entorhinal cortex suggesting a restricted, age-related cellular process affecting a specific subdomain of the apical dendrites of the granule cells (Gazzaley *et al.*, 1996, 1997). This finding is fully consistent with the changes in spine densities and in local dendritic morphology reported in the present study.

In conclusion, all of these studies point to the fact that brain aging is accompanied by rather subtle morphological and molecular changes at the level of single neuronal populations, with the spines and related synapses the major site of regressive events affecting circuit integrity. Because spines serve as the basic functional units of neuronal integration (Yuste and Denk, 1995; Shepherd, 1996; Nimchinsky *et al.*, 2002), it is possible that the memory and cognitive decline occurring during aging is related to loss of spines in neurons subserving identifiable neocortical association circuits. Future studies are needed to address this question directly in behaviorally tested animals and to explore the functional integrity of synapses during aging.

## Notes

We thank Drs E.A. Nimchinsky, P.R. Rapp and G.N. Elston for helpful discussion, Dr Y. He and B. Wicinski, W.G.M. Janssen, G. Volmar, and R. Jenkins for help with animal surgery and postoperative care, Dr J.M. Erwin for providing the aged animals and Dr P.R. Rapp for the young rhesus monkeys, Dr V. Haroutunian for providing the human brain specimens, A. Rodriguez, D. Ehlenberger, K.T. Kelliher, R.A. Shah, and Dr W.G. Young for software development, and T. Flores for help with graphics. P.R.H. is Regenstreif Professor of Neuroscience. This work was supported by NIH grants AG05138 and AG06647, by the Howard Hughes Medical Institute, by the American Federation for Aging Research, and by the Mount Sinai School of Medicine.

Address correspondence to Patrick R. Hof, Kastor Neurobiology of Aging Laboratories, Box 1639, One Gustave L. Levy Place, Mount Sinai School of Medicine, New York, NY 10029, USA. Email: patrick.hof@mssm.edu.

## References

- Anderson B, Rutledge V (1996) Age and hemisphere effects on dendritic structure. *Brain* 119:1983–1990.
- Barbas H (1986) Pattern in the laminar origin of corticocortical connections. *J Comp Neurol* 252:415–422.
- Barbas H, Mesulam MM (1985) Cortical afferent input to the principal region of the rhesus monkey. *Neuroscience* 15:619–637.
- Benavides-Piccione R, Ballesteros-Yáñez I, DeFelipe J, Yuste R (2002) Cortical area and species differences in dendritic spine morphology. *J Neurocytol* 31:337–346.
- Boothe RG, Greenough WT, Lund JS, Wrege K (1979) A quantitative investigation of spine and dendrite development of neurons in visual cortex (area 17) of *Macaca nemestrina* monkeys. *J Comp Neurol* 186:473–489.
- Bourgeois JP, Rakic P (1993) Changes in synaptic density in the primary

- visual cortex of the macaque monkey from fetal to adult stage. *J Neurosci* 13:2801–2820.
- Bourgeois JP, Goldman-Rakic PS, Rakic P (1994) Synaptogenesis in the prefrontal cortex of rhesus monkey. *Cereb Cortex* 4:78–96.
- Bressler SL (1995) Large-scale cortical networks and cognition. *Brain Res Rev* 20:288–304.
- Buell SJ, Coleman PD (1979) Dendritic growth in the aged human brain and failure of growth in senile dementia. *Science* 206:854–856.
- Buell SJ, Coleman PD (1981) Quantitative evidence for selective dendritic growth in normal human aging but not in senile dementia. *Brain Res* 214:23–41.
- Coleman PD, Flood DG (1987) Neuron numbers and dendritic extent in normal aging and Alzheimer's disease. *Neurobiol Aging* 8:521–545.
- Cupp CJ, Uemura E (1980) Age-related changes in prefrontal cortex of *Macaca mulatta*: quantitative analysis of dendritic branching patterns. *Exp Neurol* 69:143–163.
- Cusick CG, Seltzer B, Cola M, Griggs E (1995) Chemoarchitectonics and corticocortical terminations within the superior temporal sulcus of the rhesus monkey: evidence for subdivisions of superior temporal polysensory cortex. *J Comp Neurol* 360:513–535.
- de Brabander JM, Kramers RJ, Uylings HB (1998) Layer-specific dendritic regression of pyramidal cells with ageing in the human prefrontal cortex. *Eur J Neurosci* 10:1261–1269.
- de Lima, AD, Voigt T, Morrison, JH (1990) Morphology of the cells within the inferior temporal gyrus that project to the prefrontal cortex in the macaque monkey. *J Comp Neurol* 296:159–172.
- Duan H, He Y, Wicinski B, Morrison JH, Hof PR (2000) Age-related dendrite and spine changes in corticocortically projecting neurons in macaque monkeys. *Soc Neurosci Abstr* 26:1237.
- Duan H, Wearne SL, Morrison JH, Hof PR (2002) Quantitative analysis of the dendritic morphology of corticocortical projection neurons in the macaque monkey association cortex. *Neuroscience* 114:349–359.
- Elston GN (2000) Pyramidal cells of the frontal lobe: all the more spinous to think with. *J Neurosci* 20:RC95.
- Elston GN (2003) Pyramidal cell heterogeneity in the visual cortex of the nocturnal New World owl monkey (*Aotus trivirgatus*). *Neuroscience* 117:213–219.
- Elston GN, DeFelipe J (2002) Spine distribution in cortical pyramidal cells: a common organizational principle across species. In: Changing views of Cajal's neuron (Azmitia EC, DeFelipe J, Jones EG, Rakic P, Ribak CE, eds), *Progress in Brain Research* Vol. 136, pp. 109–133. Amsterdam: Elsevier.
- Elston GN, Rosa MG (2000) Pyramidal cells, patches, and cortical columns: a comparative study of infragranular neurons in TEO, TE, and the superior temporal polysensory area of the macaque monkey. *J Neurosci* 20:RC117.
- Elston GN, Benavides-Piccione R, DeFelipe J (2001) The pyramidal cell in cognition: a comparative study in human and monkey. *J Neurosci* 21:RC163.
- Feldman ML, Dowd C (1975) Loss of dendritic spines in aged cerebral cortex. *Anat Embryol* 148:279–301.
- Feldman ML, Peters A (1979) A technique for estimating total spine numbers on Golgi-impregnated dendrites. *J Comp Neurol* 188:527–542.
- Felleman DJ, Van Essen DC (1991) Distributed hierarchical processing in the primate cerebral cortex. *Cereb Cortex* 1:1–47.
- Fooden J (1976) Provisional classification and key to living species of macaques (Primates: *Macaca*). *Folia Primatol* 25:225–236.
- Fuster JM (1997) Network memory. *Trends Neurosci* 20:451–459.
- Gallagher M, Rapp PR (1997) The use of animal models to study the effects of aging on cognition. *Annu Rev Psychol* 48:339–370.
- Gazzaley AH, Siegel SJ, Kordower JH, Mufson EJ, Morrison JH (1996) Circuit-specific alterations of *N*-methyl-D-aspartate receptor subunit 1 in the dentate gyrus of aged monkeys. *Proc Natl Acad Sci USA* 93:3121–3125.
- Gazzaley AH, Thakker MM, Hof PR, Morrison JH (1997) Preserved number of entorhinal cortex layer II neurons in aged macaque monkeys. *Neurobiol Aging* 18:549–553.
- Goldman-Rakic PS (1988). Topography of cognition: parallel distributed networks in primate association cortex. *Annu Rev Neurosci* 11:137–156.
- Groves C (2001) Primate taxonomy. Washington, DC: Smithsonian Institution Press.
- Harris KM, Kater SB (1994) Dendritic spines: cellular specializations imparting both stability and flexibility to synaptic function. *Annu Rev Psychol* 17:341–371.
- Harrison KH, Hof PR, Wang SSH (2002) Scaling laws in the mammalian neocortex: does form provide clues to function? *J Neurocytol* 31:289–298.
- Henry BI, Hof PR, Rothnie P, Wearne SL (2001) Fractal analysis of aggregates of non-uniformly sized particles: an application to macaque monkey cortical pyramidal neurons. In: Emergent nature – patterns, growth and scaling in the sciences (Nowak MM, ed.), pp. 65–75. Singapore: World Scientific.
- Hof PR, Cox K, Morrison JH (1990) Quantitative analysis of a vulnerable subset of pyramidal neurons in Alzheimer's disease: I. Superior frontal and inferior temporal cortex. *J Comp Neurol* 301:44–54.
- Hof PR, Nimchinsky EA, Morrison JH (1995) Neurochemical phenotype of corticocortical connections in the macaque monkey: quantitative analysis of a subset of neurofilament protein-immunoreactive projection neurons in frontal, parietal, temporal, and cingulate cortices. *J Comp Neurol* 362:109–133.
- Hof PR, Nimchinsky EA, Young WG, Morrison JH (2000) Numbers of Meynert and layer IVB cells in area V1: a stereologic analysis in young and aged macaque monkeys. *J Comp Neurol* 420:113–126.
- Hof PR, Duan H, Page TL, Einstein M, Wicinski B, He Y, Erwin JM, Morrison JH (2002) Age-related changes in GluR2 and NMDAR1 glutamate receptor subunit protein immunoreactivity in corticocortically projecting neurons in macaque and patas monkeys. *Brain Res* 928:175–186.
- Horner CH (1993) Plasticity of the dendritic spine. *Prog Neurobiol* 41:281–321.
- Huttenlocher PR (1979) Synaptic density in human frontal cortex – developmental changes and effects of aging. *Brain Res* 163:195–205.
- Jacobs B, Scheibel AB (1993) A quantitative dendritic analysis of Wernicke's area in humans. I. Lifespan changes. *J Comp Neurol* 327:83–96.
- Jacobs B, Driscoll L, Schall M (1997) Life-span dendritic and spine changes in areas 10 and 18 of human cortex: a quantitative Golgi study. *J Comp Neurol* 386:661–680.
- Jacobs B, Schall M, Prather M, Kapler E, Driscoll L, Baca S, Jacobs J, Ford K, Wainwright M, Trembl M (2001) Regional dendritic and spine variation in human cerebral cortex: a quantitative Golgi study. *Cereb Cortex* 11:558–571.
- Jones EG, Powell TPS (1970) An anatomical study of converging sensory pathways within the cerebral cortex of the monkey. *Brain* 93:793–820.
- Lund JS, Boothe RG, Lund RD (1977) Development of neurons in the visual cortex (area 17) of the monkey (*Macaca nemestrina*): a Golgi study from fetal day 127 to postnatal maturity. *J Comp Neurol* 176:149–188.
- Melchitzky DS, Sesack SR, Pucak ML, Lewis DA (1998) Synaptic targets of pyramidal neurons providing intrinsic horizontal connections in monkey prefrontal cortex. *J Comp Neurol* 390:211–224.
- Mesulam MM (1998) From sensation to cognition. *Brain* 121:1013–1052.
- Miller EK, Cohen JD (2001) An integrative theory of prefrontal cortex function. *Annu Rev Neurosci* 24:167–202.
- Morrison JH, Hof PR (1997) Life and death of neurons in the aging brain. *Science* 278:412–419.
- Moscovitch M, Winocur G (1995) Frontal lobes, memory, and aging. *Ann NY Acad Sci* 769:119–150.
- Nakamura S, Akiguchi I, Kameyama M, Mizuno N (1985) Age-related changes of pyramidal cell basal dendrites in layers III and V of human motor cortex: a quantitative Golgi study. *Acta Neuropathol* 65:281–284.
- Nimchinsky EA, Hof PR, Young WG, Morrison JH (1996) Neurochemical, morphologic, and laminar characterization of cortical projection neurons in the cingulate motor areas of the macaque monkey. *J Comp Neurol* 374:136–160.
- Nimchinsky EA, Young WG, Yeung G, Shah RA, Gordon JW, Bloom FE, Morrison JH, Hof PR (2000) Differential vulnerability of oculomotor, facial, and hypoglossal nuclei in G86R superoxide dismutase transgenic mice. *J Comp Neurol* 416:112–125.
- Nimchinsky EA, Sabatini BL, Svoboda K (2002) Structure and function of dendritic spines. *Annu Rev Physiol* 64:313–353.
- O'Donnell KA, Rapp PR, Hof PR (1999) Preservation of prefrontal cortical volume in behaviorally characterized aged macaque monkeys. *Exp Neurol* 160:300–310.
- Page TL, Einstein M, Duan H, He Y, Flores T, Rolshud D, Erwin JM, Wearne SL, Morrison JH, Hof PR (2002) Morphological alterations in neurons

- forming corticocortical projections in the neocortex of aged Patas monkeys. *Neurosci Lett* 317:37-41.
- Peters A, Nigro NJ, McNally KJ (1997) A further evaluation of the effect of age on striate cortex of the rhesus monkey. *Neurobiol Aging* 18:29-36.
- Peters A, Rosene DL, Moss MB, Kemper TL, Abraham CR, Tigges J, Albert MS (1996) Neurobiological bases of age-related cognitive decline in the rhesus monkey. *J Neuropathol Exp Neurol* 55:861-874.
- Peters A, Morrison JH, Rosene DL, Hyman BT (1998a) Are neurons lost from the primate cerebral cortex during normal aging? *Cereb Cortex* 8:295-300.
- Peters A, Sethares C, Moss MB (1998b) The effects of aging on layer 1 in area 46 of prefrontal cortex in the rhesus monkey. *Cereb Cortex* 8:671-684.
- Peters A, Moss MB, Sethares C (2001) The effects of aging on layer 1 of primary visual cortex in the rhesus monkey. *Cereb Cortex* 11:93-103.
- Petrides M, Pandya DN (1988) Association fiber pathways to the frontal cortex from the superior temporal region in the rhesus monkey. *J Comp Neurol* 273:52-66.
- Pucak ML, Levitt JB, Lund JS, Lewis DA (1996) Patterns of intrinsic and associational circuitry in monkey prefrontal cortex. *J Comp Neurol* 376:614-630.
- Rapp PR, Gallagher M (1997) Toward a cognitive neuroscience of normal aging. *Adv Cell Aging Gerontol* 2:1-21.
- Rempel-Clower NL, Barbas H (2000) The laminar pattern of connections between prefrontal and anterior temporal cortices in the Rhesus monkey is related to cortical structure and function. *Cereb Cortex* 10:851-865.
- Rodriguez A, Ehlenberger D, Kelliher K, Einstein M, Henderson SC, Morrison JH, Hof PR, Wearne SL (2003) Automated reconstruction of 3D neuronal morphology from laser scanning microscopy images. *Methods* 30:94-105.
- Scheibel ME, Lindsay RD, Tomiyasu U, Scheibel AB (1975) Progressive dendritic changes in aging human cortex. *Exp Neurol* 47:392-403.
- Seltzer B, Pandya DN (1989) Frontal lobe connections of the superior temporal sulcus in the rhesus monkey. *J Comp Neurol* 281:97-113.
- Shepherd GM (1996) The dendritic spine: a multifunctional integrative unit. *J Neurophysiol* 75:2197-2210.
- Sholl DA (1953) Dendritic organization of the neurons of the visual and motor cortices of the cat. *J Anat* 87:387-406.
- Soloway AS, Pucak ML, Melchitzky DS, Lewis DA (2002) Dendritic morphology of callosal and ipsilateral projection neurons in monkey prefrontal cortex. *Neuroscience* 109:461-471.
- Trommald M, Jensen V, Andersen P (1995) Analysis of dendritic spines in rat CA1 pyramidal cells intracellularly filled with a fluorescent dye. *J Comp Neurol* 353:260-274.
- Uemura E (1980) Age-related changes in prefrontal cortex of *Macaca mulatta*: synaptic density. *Exp Neurol* 69:164-172.
- Uylings HB, Ruiz-Marcos A, van Pelt J (1986) The metric analysis of three-dimensional dendritic tree patterns: a methodological review. *J Neurosci Methods* 18:127-151.
- West RL (1996) An application of prefrontal cortex function theory to cognitive aging. *Psychol Bull* 120:272-292.
- Young MP (1993) The organization of neural systems in the primate cerebral cortex. *Proc R Soc Lond B Biol Sci* 252:13-18.
- Yuste R, Denk W (1995) Dendritic spines as basic functional units of neuronal integration. *Nature* 375:682-684.
- Zecevic N, Bourgeois JP, Rakic P (1989) Changes in synaptic density in motor cortex of rhesus monkey during fetal and postnatal life. *Dev Brain Res* 50:11-32.